Available online at www.sciencedirect.com
ScienceDirect
International Journal of Thermal Sciences 46 (2007) 501–505
International Journal of Thermal Sciences
www.elsevier.com/locate/ijts

Augmentation of heat transfer in a channel using a triangular prism

Himadri Chattopadhyay *

Central Mechanical Engineering Research Institute, Durgapur 713209, India

Received 16 February 2006; received in revised form 4 July 2006; accepted 4 July 2006

Available online 14 August 2006

Abstract

Heat transfer in a channel in presence of a triangular prism has been numerically investigated in the turbulent flow regime up to the Reynolds number of 40 000. The aspect ratio of channel to the prism element was fixed at 4.0. The Navier–Stokes equation along with the energy equation has been solved using SIMPLE technique and the standard k–ε formulation was chosen for turbulence closure. While a structured rectangular grid was used over the entry and exit regions, the area adjacent to the prism element was discretized using an unstructured triangular mesh. The results indicate that in presence of a triangular element, heat transfer in a channel is augmented by around 15%. The enhancement in heat transfer is related to the vortex formation downstream of the prism element. However, the augmentation is associated with higher values of skin friction coefficient on the channel wall.

Keywords: Triangular prism; Heat transfer; Augmentation; Turbulent; Numerical

1. Introduction

Augmentation of heat transfer is a subject of considerable interest to researchers [1] as it leads to savings in energy and cost. There exist numerous applications of heat transfer in channels in process industries and engineering systems. Enhancing transport processes in such channels is naturally a point of concern. These are of particular relevance in design of heat exchangers. Enhancement in heat transfer using different geometries such as vortex generators in the form of delta wing or winglet pair or by insertion of twisted tapes has been tried. Flow around bluff bodies such as cylinder and square cylinder has also been studied in detail due to their practical relevance.

A triangular prism element is very basic configuration as a bluff body though its role has not been studied in detail. Abbassi et al. [2] indicated that use of a prism could enhance the heat transfer in a channel. However their numerical study using FEM was limited to the laminar regime. They found that at around $Re = 100$, significant enhancement in heat transfer can be obtained using a triangular prism (TP). Significant enhancement was discerned only after the flow field was periodic. The presence of any bluff body in the flow field generates longitudinal vortices which promotes mixing and thereby enhances heat transfer [3]. Effect of the presence of bodies with different shapes was investigated by Jackson [4] through finite element simulation. It is worth mention that the advent of CFD has helped to investigate flow field in complex situations using the desktop computers. A first-hand estimate of the transport variables could be easily made which of course should be subject to rigorous validation.

In the present work, simulation of turbulent flow and heat transfer in a two-dimensional channel with a TP placed inside was performed. The aspect ratio of the prism, i.e. the ratio of the channel height and the prism base edge was 0.25. The sides of the prism form an equilateral triangle. While the channel length was $32B$, the location of the prism was maintained at $x = 8B$. This configuration was closer to the geometry of Abbassi et al. [2] which was used as a benchmark for validation.

2. Mathematical model

It was assumed that the flow is incompressible with constant properties. The working fluid was air with $Pr = 0.71$. The non-dimensional Reynolds-averaged Navier–Stokes (RANS) equations with rotational symmetry are provided below. For

* Tel.: +91 3432546818; fax: +91 343 2546505.
E-mail address: chimadri@rediffmail.com (H. Chattopadhyay).

1290-0729/$ – see front matter
doi:10.1016/j.ijthermalsci.2006.07.003

Nomenclature

B	base of the prism
C_f	skin friction coefficient
H	height of the computational domain
k	kinetic energy of turbulence
L	length of domain in x direction
Nu	Nusselt number
p	pressure
Pr	Prandtl number
Re	Reynolds number
T	temperature
u	mean velocity component in x direction
u_{in}	inlet velocity
w	mean velocity component in z direction

Greek symbols

ν	kinematic viscosity
τ	shear stress

Subscripts

av	average
asy	asymptotic
in	inlet
TP	triangular prism
∞	ambience

non-dimensionalization, the characteristics length and velocity is H and u_{in}, respectively. The pressure and temperature has been non-dimensionalized by $p = p^*/2\rho u_{\text{in}}^2$ and $T = (T^* - T_\infty)/(T_w - T_\infty)$, respectively. Here * denotes dimensional quantity.

Continuity equation:

$$\frac{\partial u}{\partial x} + \frac{\partial w}{\partial z} = 0 \tag{1}$$

Momentum equation in x-direction:

$$\frac{\partial}{\partial x}(uu) + \frac{\partial}{\partial z}(uv) = -\frac{\partial p}{\partial x} + \frac{1}{Re}\left(1 + \frac{\nu_t}{\nu}\right)\nabla^2 u \tag{2}$$

Momentum equation in z-direction:

$$\frac{\partial}{\partial x}(uw) + \frac{\partial}{\partial z}(ww) = -\frac{\partial p}{\partial z} + \frac{1}{Re}\left(1 + \frac{\nu_t}{\nu}\right)\nabla^2 w \tag{3}$$

Energy equation:

$$u\frac{\partial T}{\partial x} + v\frac{\partial T}{\partial z} = \frac{1}{Re\,Pr}\left(1 + \frac{\alpha_t}{\alpha}\right)\nabla^2 T \tag{4}$$

The turbulent viscosity term ν_t is to be computed from an appropriate turbulence model. The expression for the turbulent viscosity is given as:

$$\upsilon_t = C_\mu Re\frac{k^2}{\varepsilon} \tag{5}$$

The turbulent diffusivity is related to the molecular diffusivity in the following manner

$$Re\,Pr\frac{\nu_t}{\alpha_t} = Pr_t \tag{6}$$

The value of turbulent Prandtl number Pr_t is chosen as 0.85.

For closing the time-averaged momentum equation, the k–ε model [5] was chosen. Despite its limitations, this model has been successfully applied to flows with engineering applications including flows in channels. Deb et al. [6] reported successful application of k–ε model in predicting transport processes in a channel in presence of a triangle-shaped vortex generator. Since the three-dimensional flow field was captured efficiently by them using the standard k–ε model, it is assumed to be appropriate for the present simulation which is two-dimensional in nature.

The equations for k and ε are given as:

$$u\frac{\partial k}{\partial x} + w\frac{\partial k}{\partial z} = \frac{1}{Re}\left(1 + \frac{\nu_t}{\sigma_k}\right)\nabla^2 k + P - \varepsilon \tag{7}$$

$$u\frac{\partial \varepsilon}{\partial x} + w\frac{\partial \varepsilon}{\partial z} = \frac{1}{Re}\left(1 + \frac{\nu_t}{\sigma_\varepsilon}\right)\nabla^2 \varepsilon - C_1 S\varepsilon - \rho C_2\frac{\varepsilon^2}{k} \tag{8}$$

where P is the production of turbulent kinetic energy. The model coefficients are given below and adapted from Launder and Spalding [5] and was reported to work well in flow fields dominated by longitudinal vortices [6]

$$\sigma_k = 1.0 \quad \text{and} \quad \sigma_\varepsilon = 1.2, \quad C_{1\varepsilon} = 1.44, \quad C_2 = 1.9$$

At the inlet uniform velocity profile ($u = u_{\text{in}}$) has been imposed. Impermeable boundary condition (i.e. $u = w = 0$) has been implemented over the channel wall as well as the TP. The turbulence intensity was kept at 10% at the inlet, unless otherwise stated.

The non-dimensional temperature of the bottom plate was taken as unity (i.e. $T_s = 1.0$) and the inlet temperature was assumed at the ambient level (i.e. $T_{\text{in}} = 0.0$). The TP was maintained at adiabatic condition so that $\partial T/\partial n = 0$ where n is the normal to the TP surface.

The governing equations were solved using the SIMPLE formulation [7] using the commercial code FLUENT [8]. The solutions were considered to converge when the normalized residual values were 10^{-7} for the temperature and 10^{-5} for the other variables.

3. Results and discussions

While the channel could be easily resolved into regular grids, the presence of TP requires deployment of irregular grid. Therefore, the entire computation domain was splitted in to three parts. The entry region and the exit region were resolved by regular Cartesian elements. The intermediate regime containing the TP was resolved with triangular unstructured meshes. For the case of plane channel, however, regular grid was applied throughout the domain. Grid independent solution was obtained

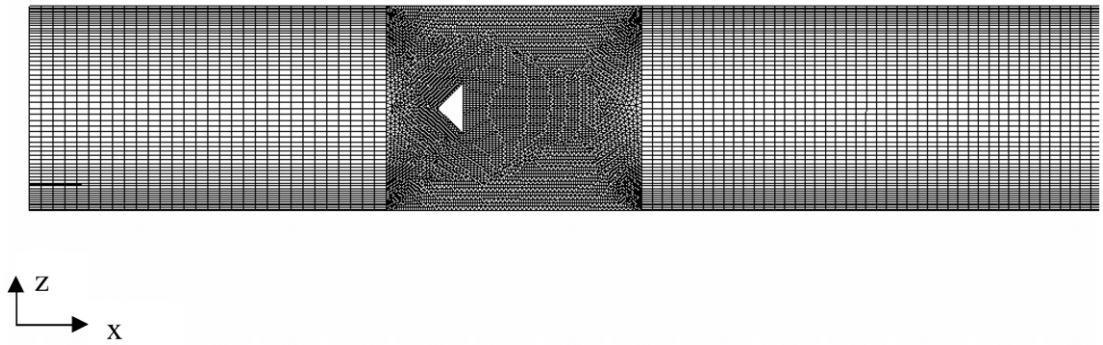

Fig. 1. Grid arrangements for the channel with the triangular prism.

by comparing the solution for different grid levels. The total number of nodes were 15 410 and 10 800 for the cases with and without TP, respectively. The higher number of nodes when the TP is present is due to triangular meshes employed around the TP with finer resolution near the TP walls, as shown in Fig. 1. The plane channel flow was also simulated with a 2-D code developed by the author [9] for simulation of pulsating flow. This code uses SIMPLE algorithm with momentum interpolation technique due to Rhie and Chow [10]. The distribution of skin friction coefficient from this code agreed within 2% with the results of FLUENT. Thus the use of the commercial code was validated against an in-house code. In case of a plane channel the present work reports the value of Nu as 30.97 while the value from Dittus–Boelter correlation is 63.5. It can be mentioned here that the correlation is based on hydraulic diameter and for a 2-D channel considered to be infinitely extended in the third direction, the hydraulic diameter is two times the channel height and hence the difference with correlation is only by 0.25%.

Two parameters of interest for the present case are the skin friction coefficient and the Nusselt number.

The skin friction coefficient C_f is given by

$$C_f = \frac{\tau_s}{\frac{1}{2}\rho w_\infty^2}$$

Under the present scheme of non-dimensionalization, the term can be finally calculated as the gradient of velocity, i.e.:

$$C_f \cdot Re = \frac{\partial v}{\partial z}$$

The heat transfer performance is measured by Nusselt number which can be found by the local temperature gradient as:

$$Nu = -\frac{\partial T}{\partial z}$$

The average Nusselt number can be obtained by $Nu_{\text{av}} = \int Nu(x)\partial x/L$ where L is the length of the computational domain.

The time-averaged flow structure in presence of a TP could be easily discerned by looking at the velocity vector plots at Fig. 2. Here the velocity field around the TP is presented. It can be seen that the flow stream divides itself in two streams as it hits the TP and combines after the TP. However, two counter-rotating pair of vortices are clearly observed at the location

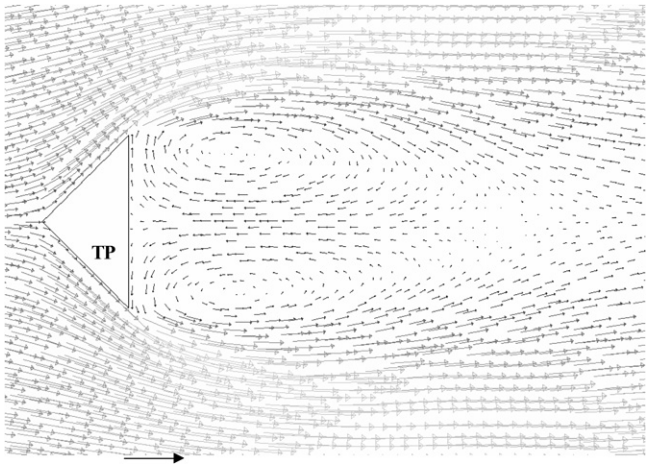

Fig. 2. Velocity vectors around the TP.

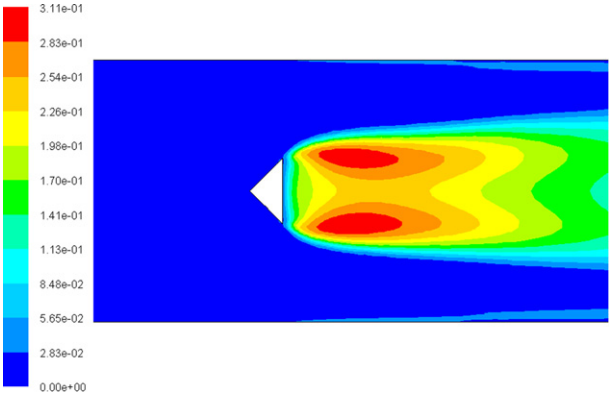

Fig. 3. Contours of turbulent kinetic energy k at $Re = 20\,000$.

immediately following the TP. Such vortices are also discernable for other types of vortex generators such as delta wings and winglet pairs [3]. The contours of turbulent kinetic energy is presented in Fig. 3. The TP is found to produce a highly turbulent filed as reflected in the high values of k around 25%. Two zones of high turbulence correspond to the two vortices observed in Fig. 2. These zones are about 2–3B downstream the location of the base of the TP.

In Fig. 4, Nu for the case with TP is compared with the case of a plane channel at $Re = 20\,000$. It can be observed here that Nu increases immediately after the location of the TP. There

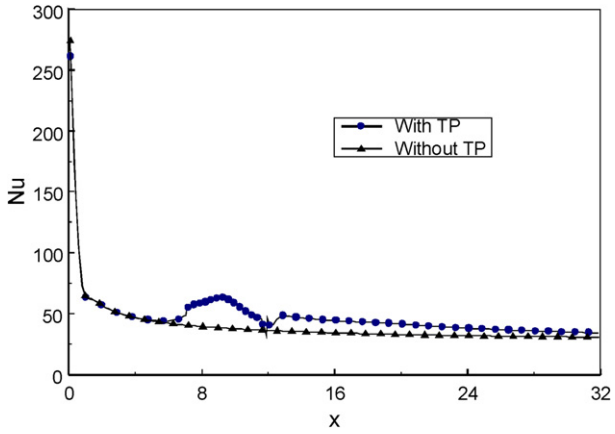

Fig. 4. Distribution of *Nu* at $Re = 20\,000$.

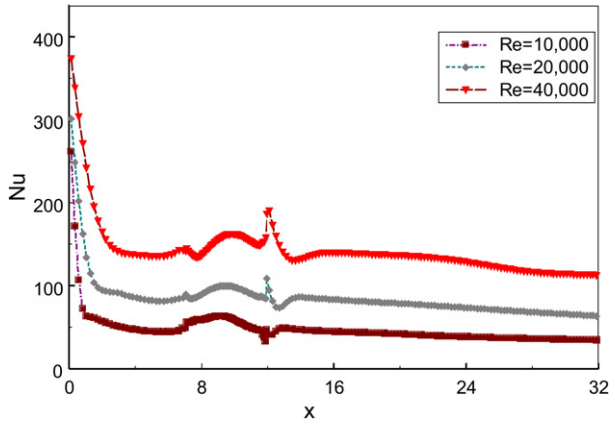

Fig. 5. Distribution of *Nu* along the channel wall.

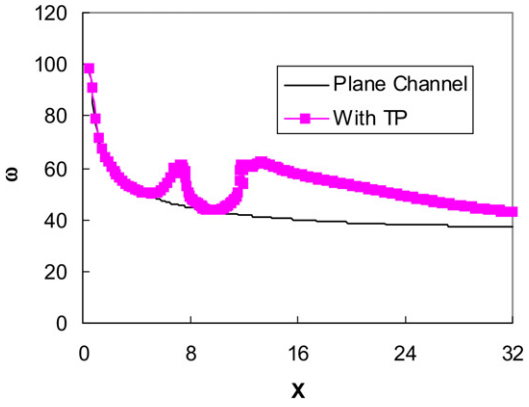

Fig. 6. Distribution of vorticity magnitude at $z = 0.005$.

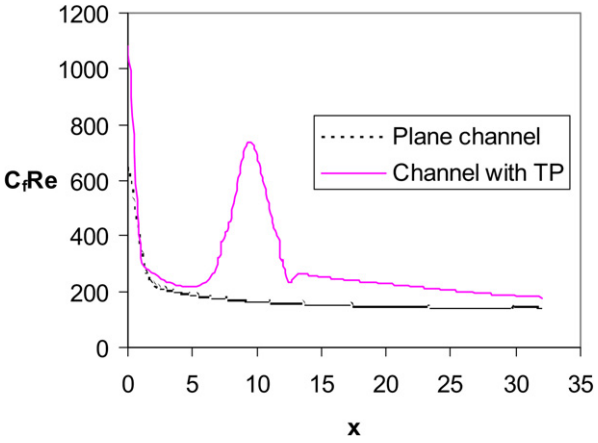

Fig. 7. Distribution of skin friction coefficient at $Re = 20\,000$.

occur a secondary peak and a crest further downstream. At the exit region, the asymptotic *Nu* value is found to be higher when the TP is present.

Heat transfer distributions at different *Re* in presence of the TP is shown in Fig. 5. It can be discerned here that the patterns are similar. However the magnitude of heat transfer increases at increased *Re*. At $Re = 20\,000$ and $40\,000$, second peaks are higher in magnitude compared to first peak following the TP. A scale analysis showed that the asymptotic *Nu* scales with $Re^{0.85}$.

Fig. 6 shows the distribution of non-dimensional vorticity for the cases with and without a TP, at $z = 0.005$, which is very close to the wall. At the location immediately following the TP, the vorticity level is higher in presence of a TP as compared to the case of a plane channel. The vorticity distribution curve shows two peaks and one crest in the zone which follows the TP, but eventually the vorticity level downstream the TP is always higher compared to the case of a plane channel. The vorticity level at the exit plane is higher by about 15% when the TP is present. Thus the generation of vortices due to the TP as well as the role of turbulence in better mixing brings in the augmentation in heat transfer from the channel wall.

Table 1 summarizes the heat transfer data. It can be observed from the table that average *Nu* increases by about 17% in the duct when a TP is present. Similarly, the heat transfer downstream the channel, as reflected in Nu_{asy} increases by about 12% due to the TP element. It may be recalled that the increase in the vorticity was about 15% at the channel exit establishing the relationship between the heat transfer enhancement. Thus insertion of TP helps in bringing augmentation all through the channel and the effect is even noticeable at the far downstream region.

Table 1
Comparison of heat transfer

Re_H	Nu_{av}	$Nu_{av,TP}$	Enhancement [%]	Nu_{asy}	$Nu_{av,TP}$	Enhancement [%]
10 000	43.05	50.89	18.21	30.97	34.13	10.2
20 000	77.35	91.11	17.78	55.89	63.46	13.54
40 000	130.23	152.11	16.72	98.38	111.97	13.81

Suffixes av, TP and asy denoted averaged, triangular prism and asymptotic, respectively.

Finally, it is well known that the enhancement in heat transfer is associated with penalty in terms if increased skin friction coefficient leading to higher pressure drop. The distributions of $C_f Re$ is presented in Fig. 7, where it is evident that the presence of the TP involves increased value of surface friction on the channel wall. The rise of C_f following the TP persists even at far downstream location. While the change is more that 200% at the locations corresponding to the zones of counter rotating vortex pairs, the enhancement in C_f at the channel exit is about

25% compared to the case of a developing turbulent flow in a plane channel.

4. Concluding remarks

Estimate of heat transfer enhancement in a channel due to the presence of a triangular element was obtained using numerical simulation. The order of enhancement is about 15%. However, as expected, the augmentation is associated with enhanced skin friction. The effect of aspect ratio of the prism, density variation and three-dimensionality of the flow field in case of a finite TP are some of the important aspects, which were not addressed in the present work and is planned to be investigated in future.

References

[1] A.E. Bergles, Techniques to augment heat transfer, in: Handbook of Heat Transfer Applications, McGraw-Hill, New York, 1983, pp. 31–80.

[2] H. Abbassi, S. Turki, S. Ben Nasrallah, Numerical investigation of forced convection in a horizontal channel with a built-in triangular prism, ASME J. Heat Transfer 124 (2002) 571–573.

[3] G. Biswas, H. Chattopadhyay, Heat transfer in a channel with built-in wing type vortex generators, Int. J. Heat Mass Transfer 35 (1992) 803–814.

[4] C.P. Jackson, A finite element study of the onset of vortex shedding in flow past variously shaped bodies, J. Fluid Mech. 365 (1987) 23–45.

[5] B.E. Launder, D.B. Spalding, Lectures in Mathematical Models of Turbulence, Academic Press, London, 1972.

[6] P. Deb, G. Biswas, N.K. Mitra, Heat transfer and flow structure in laminar and turbulent flows in a rectangular channel with longitudinal vortices, Int. J. Heat Mass Transfer 38 (1995) 2427–2444.

[7] H. Chattopadhyay, F. Durst, S. Ray, Analysis of heat transfer in simultaneously developing pulsating laminar flow in a pipe with constant wall temperature, Int. Comm. Heat Mass Transfer 33 (2006) 475–481.

[8] Fluent Inc., Users Manual—FLUENT 6.0, Lebanon, 2002.

[9] S.V. Patankar, Numerical Heat Transfer and Fluid Flow, Hemisphere, Washington, DC, 1980.

[10] C.M. Rhie, W.L. Chow, Numerical study of the turbulent flow past an airfoil with trailing edge separation, AIAA J. 21 (11) (1983) 1525–1532.